

Supporting Information for

Benchmark selectivity *p*-xylene separation by a non-porous molecular solid through liquid or vapor extraction

Na Sun^a, Shi-Qiang Wang^c, Ruqiang Zou^a, Wengang Cui^b, Anqi Zhang^a, Tianzhen Zhang^a, Qi Li^b,
Zhanzhong Zhuang^a, Yinghui Zhang^b, Jialiang Xu^{*b}, Michael J. Zaworotko^c, Xian-He Bu^{*a,b}

^a State Key Laboratory of Elemento-Organic Chemistry, College of Chemistry, Nankai University,
Tianjin 300071, China.

^b School of Materials Science and Engineering, National Institute for Advanced Materials, TKL of
Metal and Molecule-Based Material Chemistry, Nankai University, Tianjin 300350, China.

^c Department of Chemical Sciences and Bernal Institute, University of Limerick, Limerick, Republic of
Ireland.

E-mail: *buxh@nankai.edu.cn; jialiang.xu@nankai.edu.cn

Table of Contents

Section A. Materials and Instrumentation	3
Single Crystal X-ray Diffraction (SCXRD).....	3
Powder XRD (PXRD).....	3
Nuclear Magnetic Resonance (NMR) Spectra.....	3
Thermogravimetric Analysis (TGA).....	3
Ultraviolet Spectrum (UV)	4
Dynamic Vapor Sorption (DVS)	4
Gas Chromatography Analysis (GC).....	4
Section B. Synthesis of M and Its Clathrates.....	5
Synthesis of the Ligand.....	5
Synthesis of Complexes.....	5
M	5
<i>p</i> -Xylene@ M (<i>pX</i> @ M).....	5
<i>m</i> -Xylene@ M (<i>mX</i> @ M).....	5
<i>o</i> -Xylene@ M (<i>oX</i> @ M)	6
Section C. Crystallographic Data.....	8
Section D. Structure Analyses	9
The Structure Analyses of M	9
Structure Analyses of <i>pX</i> @ M , <i>mX</i> @ M , <i>oX</i> @ M	10
Section E. Xylene Isomer Selectivity Studies.....	15
Solubility of Host in Xylene	15
Xylene Selectivity Studies in Liquid	16
Recycled of M	20
Xylene Selectivity Studies in Vapor	21
DFT Calculations	25
Section F. Main Bond Length and Bond Angle.....	26
Section G. References.....	28

Section A. Materials and Instrumentation

All reagents were purchased from commercial suppliers and used without further purification.

Single Crystal X-ray Diffraction (SCXRD)

Crystal data were collected on a Rigaku XtalAB PRO MM007 DW diffractometer at 293(2) K and 100 K with Mo K α radiation ($\lambda = 0.7107 \text{ \AA}$) by the ϕ and ω scan mode. The program SAINT⁷ was used for integration of the diffraction profiles. The structures were solved by direct methods using the SHELXS program of the SHELXTL package and refined by full-matrix least-squares methods with SHELXL.¹ All hydrogen atoms attached to carbon atoms were calculated in ideal positions. The high disorder of solvent molecules led to the failure of the attempts to model and refine the solvent peaks and the diffused electron densities resulted from them were removed by the SQUEEZE routine of PLATON. All crystallographic data are available free of charge from the Cambridge Crystallographic Data Centre (CCDC) via www.ccdc.cam.ac.uk/data_request/cif.

Powder XRD (PXRD)

Powder XRD experiments were conducted using microcrystalline samples on a Rigaku D/Max-2500 diffractometer at 40 kV, 100 mA for a Cu-target tube and a graphite monochromator. A scan speed of 6.7°/min, with a step of 0.026° in 2θ was used at room temperature with a range of $5^\circ < 2\theta < 40^\circ$.

Nuclear Magnetic Resonance (NMR) Spectra

NMR spectra were recorded on a BrukerAvance 400, with working frequencies of 400 MHz. Chemical shifts are reported in ppm relative to the signals corresponding to the residual non-deuterated solvents ($(\text{CD}_3)_2\text{SO}$: $\delta_{\text{H}} = 2.54 \text{ ppm}$; CD_3CN : $\delta_{\text{H}} = 1.94 \text{ ppm}$; CDCl_3 : $\delta_{\text{H}} = 7.26 \text{ ppm}$; CD_2Cl_2 : $\delta_{\text{H}} = 5.32 \text{ ppm}$; CD_3COCD_3 : $\delta_{\text{H}} = 2.05 \text{ ppm}$; D_2O : $\delta_{\text{H}} = 4.79 \text{ ppm}$).

Thermogravimetric Analysis (TGA)

TGA for all the compounds were carried out under air atmosphere in a TA instruments Q50 thermal analyzer between room temperature and 800 °C with a constant heating rate of 5 °C/min.

Ultraviolet Spectrum (UV)

UV measurements were carried out using UV-2600. The supernatant after soaking the host **M** in xylenes for 8 hours was measured with the corresponding pure xylene as the background.

Dynamic Vapor Sorption (DVS)

Dynamic vapor sorption measurements were conducted using a Surface Measurement Systems DVS Vacuum at 298 K. To study the xylene vapor kinetics on **M**, samples of **M** were first under high vacuum (1×10^{-4} Torr) *in-situ* for 60 min and then exposed to 95% relative pressure of each xylene vapor for 750 min. The mass of the sample was determined by comparison to an empty reference pan and recorded by a high resolution microbalance with a precision of 0.1 μg .

Gas Chromatography Analysis (GC)

GC measurements were carried out using a SHIMADZU GC-2014C instrument configured with an FID detector and a SH-Rtx-Wax capillary column ($30 \text{ m} \times 0.53 \text{ mm} \times 1.00 \text{ }\mu\text{m}$). GC measurements were carried out using a SHIMADZU GC-2014C instrument configured with an FID detector and a SH-Rtx-Wax capillary column ($30 \text{ m} \times 0.53 \text{ mm} \times 1.00 \text{ }\mu\text{m}$). The standard curve is tested by the external standard method. Samples were analysed using direct injections by sampling 1 μL . The GC method was described below: the oven was programmed to heat up from 40 $^{\circ}\text{C}$ to 220 $^{\circ}\text{C}$ with an increments of 10 $^{\circ}\text{C}/\text{min}$ with 10 min hold, resulting 38 min run time in total; the injection temperature was 250 $^{\circ}\text{C}$; the detection temperature was 330 $^{\circ}\text{C}$ with hydrogen, air, and make-up flow-rates of 40, 400, and 30 mL/min respectively; helium (carrier gas) flow-rate 2.1 mL/min . The samples were injected in the split mode (20:1). Numeric integration of the resulting peaks was performed using the supplied ACD/ChemSketch and AI software package.

Section B. Synthesis of **M** and Its Clathrates

Synthesis of the Ligand

The ligand, (2,3-bis[3-(pyridin-2-yl)-1H-pyrazol-1-yl-methyl] quinoxaline), was prepared following literature procedures.² The reactions gave the ligand in a good yield, and the product was characterized by ¹H NMR, and elemental analysis.

Yield: 65%. ¹H NMR (400 MHz, CDCl₃): δ 5.98 (s, 4H), 6.93-8.56 (m, 16H). IR (KBr, cm⁻¹): 2901 w, 2878 w, 1591 s, 1566 m, 1489 s, 1458 s, 1401 m, 1362 m, 1231 s, 1143 w, 1049 s, 991 m, 860 m, 759 vs. Anal. Calcd for C₂₆H₂₀N₈ClO₄: C, 57.35; H, 3.68; N, 20.59%. Found: C, 57.38; H, 3.70; N, 20.57%.

Synthesis of Complexes

M

Single crystals of the **M** complex were prepared by the solvothermal reaction of AgClO₄•H₂O (24.8 mg, 0.11 mmol) and the ligand 2,3-bis[3-(pyridin-2-yl)-1H-pyrazol-1-yl-methyl] quinoxaline (44.4 mg, 0.1 mmol) in a binary solvent of water and methanol.² The temperature of the solution was programmed to raise up to 373K in 6 hours and remained for 72 hours, followed by a cooling program till room temperature in 24 hours, and then the colorless block crystals were collected. Yield: 61%. Anal. Calcd for C₂₆H₂₀AgN₈ClO₄: C, 47.9; H, 3.07; N, 17.19%. Found: C, 47.86; H, 2.97; N, 17.27%.

p-Xylene@**M** (*pX*@**M**)

pX@**M** was synthesized by the solvothermal reaction of **M** (10 mg, 15.3 μmol) with *pX* (2 mL) in CH₃OH/H₂O (1:1) at 363 K for 10 hours. The temperature of the solution was programmed to raise up to 363 K in 6 hours and remained for 10 hours, followed by a cooling program till room temperature in 24 hours, and then colorless block crystals were collected, washed with CH₃OH and dried in air. Yield: 43%. Anal. Calcd for C₇₂H₇₀Ag₂Cl₂N₁₆O₈: C, 54.94; H, 4.45; N, 15.51%. Found: C, 54.85; H, 4.51; N, 15.59%.

m-Xylene@**M** (*mX*@**M**)

mX@**M** was prepared in the same synthetic procedure as that for *pX*@**M** except that *p*-xylene was replaced by *m*-xylene. Colorless block crystals were collected with a yield of 41%. Anal. Calcd for C₃₀H₂₅AgN₈ClO₄: C, 51.12; H, 3.55; N, 15.89%. Found: C,

51.19; H, 3.57; N, 15.76%.

o-Xylene@M (*oX*@M)

oX@M was prepared in the same manner. The same synthetic procedure as that for *pX*@M was used except that *p*-xylene was replaced by *o*-xylene. The colorless block crystals were collected with a yield of 42%. Anal. Calcd for C₆₈H₆₀Ag₂Cl₂N₁₆O₈: C, 53.88; H, 3.96; N, 14.78%. Found: C, 53.79; H, 4.03; N, 14.71%.

CAUTION! Perchlorate complexes of metal ions in the presence of organic ligands are potentially explosive. These materials should be handled with extreme care in small amounts.

Table S1. Physical properties of xylene isomers

Xylene Isomer	Boiling Point (°C)	Melting Point (°C)	Kinetic Diameter (Å)
<i>pX</i>	138.50	13.20	5.8
<i>mX</i>	139.10	-47.9	6.4
<i>oX</i>	144.40	-25.2	6.5
<i>eB</i>	136.2	-94.9	5.8

Table S2. The summary of adsorbents for adsorptive separation of xylene aromatics (the order is from high to low pX/oX).

Adsorbents	Dimension	Selectivity				Ref./Note
		pX/oX	pX/mX	pX/eB	mX/oX	
M (current work)	0D	24	6.19	10.36	3.93	liquid
		20.3	5.4	8.00	1.16	vapor
H/ZSM-5	3D	16.78	24.98	6.76	NA.	³
EtP6	0D	14.28	10.20	NA.	0.26	⁴
Li/ZSM-5	3D	5.98	8.21	3.98	NA.	³
[Ce(HTCPB)]	3D	5.70	4.60	2.40	1.20	⁵
Na/ZSM-5	3D	5.45	6.721	2.01	NA.	³
MOF-monoclinic	3D	4.55	2.52	5.17	NA.	⁶
K/ZSM-5	3D	3.90	3.97	1.10	NA.	³
ZIF-8	3D	3.90	1.60	NA.	2.40	⁷
BaX nanosize	3D	2.82	7.19	3.75	NA.	⁸
KaX nanosize	3D	2.43	5.36	3.22	NA.	⁹
MIL-125(Ti)-NH ₂	3D	2.20	3.00	1.6	0.97	¹⁰
EtP5	0D	1.88	2.08	NA.	1.12	⁴
MIL-140B	3D	1.8	1.6	2.10	NA.	¹¹
MOF-48	3D	1.7	1.7	1.50	NA.	¹¹
MCF-50	1D	1.60	1.30	NA.	1.30	¹²
MIL-47 (V1)	3D	0.99	2.07	1.83	0.85	¹³
HKUST-1	3D	0.83	0.89	NA.	0.92	¹⁴
MIL-47 (V)	3D	0.71	2.5	9.7	0.5	¹⁵
CAU-13	3D	0.66	1.30	NA.	0.53	¹⁶
MIL-101 (Cr)	3D	0.63	0.91	NA.	0.67	^{17, 18}
Zn(BDC)(Dabco) _{0.5}	3D	0.53	0.8	1.15	0.89	¹⁹
MIL-53(Fe)	3D	0.39	0.54	NA.	0.63	²⁰
CPO-27-Ni	3D	0.3	0.5	NA.	0.6	¹⁴
MIL-53(Ga)	3D	0.30	0.71	NA.	0.40	²¹
MIL-53(Al)	3D	0.28	0.83	NA.	0.37	²²
MIL-53(Cr)	3D	0.27	0.71	NA.	0.35	²¹
Co ₂ (dobdc)	3D	0.25	0.63	3.21	0.40	²³
MIL-53(Al)	3D	0.19	NA.	NA.	0.19	²¹
sql-1-Co-NCS	2D	0.10	0.76	7.3	0.13	²⁴
[Ni(NCS) ₂ (ppp) ₄]	0D	0.02	0.07	NA.	0.03	²⁵
MOF-5	3D	NA.	NA.	4.14	NA.	⁶
MIL-53(Al)	3D	NA.	NA.	3.10	NA.	²⁶
UiO-66	3D	NG.	0.41	NA.	0.55	²⁷
NaY microcrystalline	3D	NA.	0.38	NA.	2.86	²⁸
NaY nanocrystalline	3D	NA.	0.34	NA.	2.16	²⁸

Note: NA. refers to not available; For each material, only the best/highest values of selectivity were selected for comparison.

Section C. Crystallographic Data

Table S3. Crystallographic data of **M** and its clathrate compound.

	M	<i>pX@M</i>	<i>mX@M</i>	<i>oX@M</i>
Formula	C ₂₆ H ₂₀ AgN ₈ ClO ₄	C ₇₂ H ₇₀ Ag ₂ Cl ₂ N ₁₆ O ₈	C ₃₀ H ₂₅ AgN ₈ ClO ₄	C ₆₈ H ₆₀ Ag ₂ Cl ₂ N ₁₆ O ₈
CCDC	1889509	1889510	1889511	1889512
Formula weight	651.82	1574.09	704.90	1515.96
Temperature/K	293(2)	169(6)	100(2)	100(2)
Crystal system	Monoclinic	Monoclinic	Triclinic	Monoclinic
Space group	<i>C2/c</i>	<i>P2₁/n</i>	<i>P-1</i>	<i>P2₁/c</i>
<i>a</i> /Å	27.078(5)	14.2045(1)	10.7387(10)	13.9995(1)
<i>b</i> /Å	12.193(2)	23.0696(2)	11.8558(2)	23.1335(3)
<i>c</i> /Å	16.988(3)	20.6652(2)	12.6250(2)	20.7862(2)
α°	90	90	67.1420(10)	90
β°	110.78(3)	97.942(1)	76.6260(10)	97.723(1)
γ°	90	90	86.6820(10)	90
Volume/Å ³	5247.0(19)	6706.87(10)	1440.05(4)	6670.70(12)
Z	8	4	2	4
ρ_{calc} g/cm ³	1.650	1.544	1.626	1.509
μ /mm ⁻¹	0.920	5.997	6.910	6.010
F(000)	2624.0	3176.0	714.0	3088.0
Radiation	CuK α	CuK α	CuK α	CuK α
Reflections collected	26148	40500	14307	37953
Independent reflections	5990 [R _{int} = 0.1161, R _{sigma} = 0.1062]	13112 [R _{int} = 0.0224, R _{sigma} = 0.0214]	5659 [R _{int} = 0.0175, R _{sigma} = 0.0171]	13191 [R _{int} = 0.0276, R _{sigma} = 0.0308]
Data/restraints/parameters	5990/0/361	13112/155/937	5659/55/421	13191/46/868
Goodness-of-fit on F ²	1.063	1.053	1.042	1.060
Final R indexes [I >= 2 σ (I)]	R ₁ = 0.0883, wR ₂ = 0.1415	R ₁ = 0.0557, wR ₂ = 0.1611	R ₁ = 0.0373, wR ₂ = 0.1044	R ₁ = 0.0750, wR ₂ = 0.2077
Final R indexes [all data]	R ₁ = 0.1920, wR ₂ = 0.1728	R ₁ = 0.0599, wR ₂ = 0.1647	R ₁ = 0.0376, wR ₂ = 0.1047	R ₁ = 0.0785, wR ₂ = 0.2104

Section D. Structure Analyses

The Structure Analyses of **M**

The single crystal structure of **M** contains two independent $[\text{AgL}]^+$ units (consisting of one ligand and one silver atom) and two perchlorate anions, completing the contents of the asymmetric unit. Two N atoms on quinoxaline ring are not involved in the coordination with Ag, owing to the huge steric hindrance of the quinoxaline ring. The quinoxaline ring in the molecule and the two pyridine pyrazole rings of the terminal group are nearly perpendicular to each other (with the angle of 78.5° and 88.6° respectively). Besides, the Ag(I) interconnects with N4, N5 (from one arm of the quinoxaline ring), N7, N8 (from another arm of the quinoxaline ring) of the pyridyl rings, forming typical Ag-N distances (2.599 - 2.698 Å) and a planar geometry (170.3 - 173.7°). From the crystallographic perspective, the L-shaped compounds are formed into a spatial structure and demonstrate strong $\text{C-H}\cdots\pi$ (2.79 Å and 3.32 Å) and $\text{C-H}\cdots\text{N}$ (2.69 Å) interactions.²⁹⁻³¹

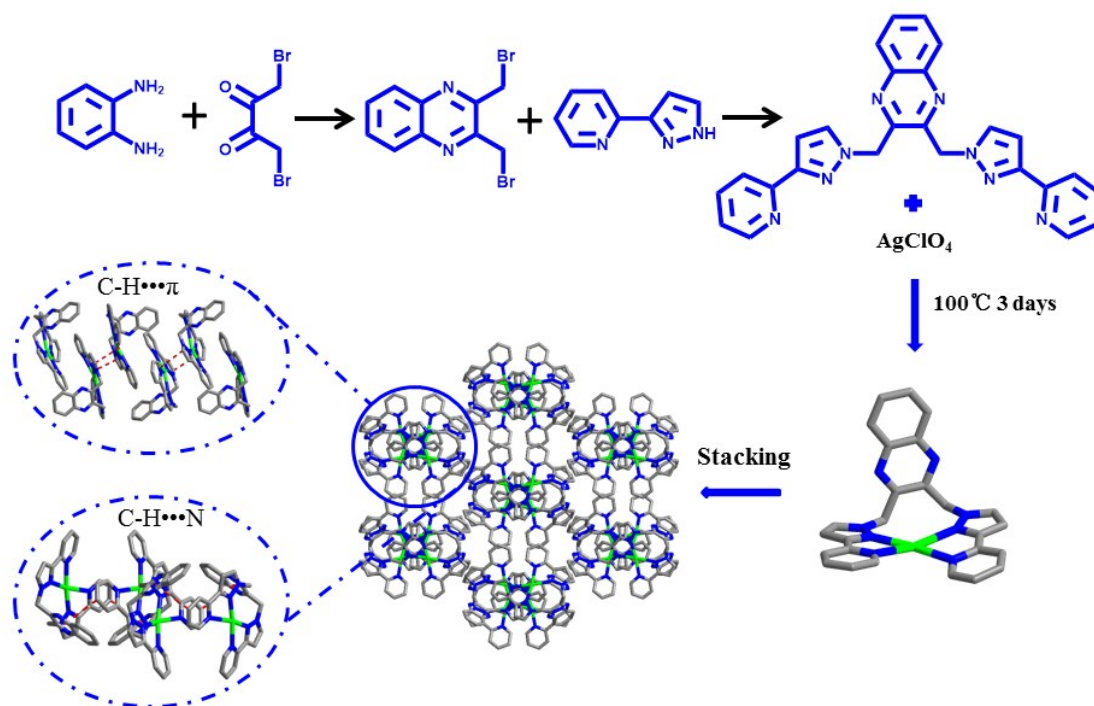


Fig. S1. Synthesis of **M** by the reaction of AgClO_4 with 2,3-bis[3-(pyridin-2-yl)-1H-pyrazol-1-yl-methyl] quinoxaline, which was formed from 1,4-dibromomethyl-2,3-butanedione, 3(2-pyridyl) pyrazole, 2S-1,2-Diaminobenzene. And three-dimensional stacking diagram of **M** by $\text{C-H}\cdots\text{N}$ and $\text{C-H}\cdots\pi$ interactions.

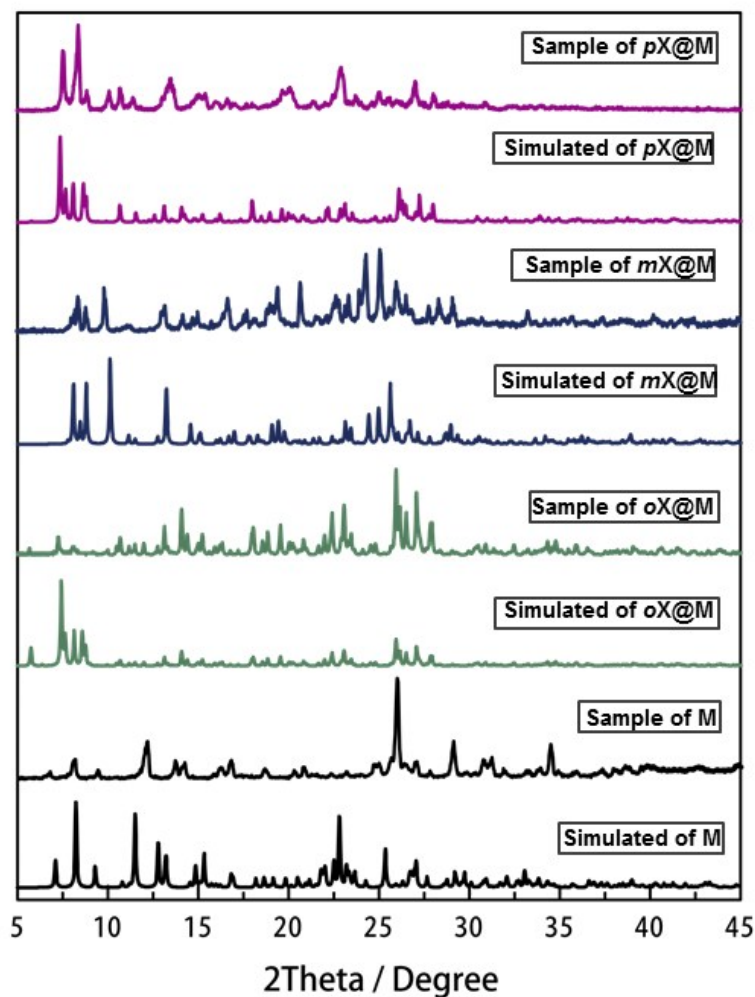


Fig. S2. Comparison of PXRD patterns of the **M**, *oX@M*, *mX@M*, *pX@M*, with simulated from single-crystal X-ray data, with the corresponding as-synthesized xylene aromatics loaded phases.

Structure Analyses of *pX@M*, *mX@M*, *oX@M*

Single crystal structures of the clathrate suggest that the compounds crystallized in monoclinic or triclinic systems. As illustrated in Fig. S3-8, the clathrate structures of xylene isomers demonstrated the overall structures underwent changes within the host-guest compounds.³²

oX and *mX* are capable of interacting with two **M** centers situated with the ligand, whereas *pX*, the compelling binding isomer. As shown in Fig. S3-4 and Table S11, the two binding sites on *pX* located on the position of methyl group and the position of aryl hydrocarbon group interact with pyridine pyrazole rings and quinoxaline ring of **M**, respectively. Other two binding sites for *pX* feature the π - π interaction at the methyl group of the inner cavity of *pX* and the external *pX* of the cavity interact with pyridine pyrazole rings. An additional binding site is the hydrogen bond for *pX* interaction with the N atom of quinoxaline ring, with C-H \cdots N distance of 2.57 Å. Particularly, as shown

the structure of $pX@M$ (Fig. 2a), one of pX is located in M cavity while the others are situated around the cavity of two adjacent M molecules. This configuration promotes the interacting connections with adjacent host molecules stronger and tighter. This is one of the main forces for selective adsorption of pX . The structure of $pX@M$ implied that pX can easily interact with M due to the size effect and the force between pX and M is much stronger.

The adsorbing isomer, mX , shown in Fig. S5-6 and Table S12, binds to two sites of M through π - π (3.45 Å) aryl C-H \cdots π (2.64 Å) and C-H \cdots O (2.62 Å) interactions, respectively. o -Xylene interacts with two sites through methyl group and aryl C-H bond (Fig. S7-8 and Table S13). The interactions of aryl C-H bond with quinoxaline ring are longer than those observed with pX , in line with the lower affinity of M for oX . It is evident that the aryl C-H \cdots π distance of pX (3.04 Å). These comparatively weaker oX interactions likely result from the additional steric bulk of the oX , which prevents a closer approach of molecule to the quinoxaline ring, accounting for the feeble affinity of oX with M .

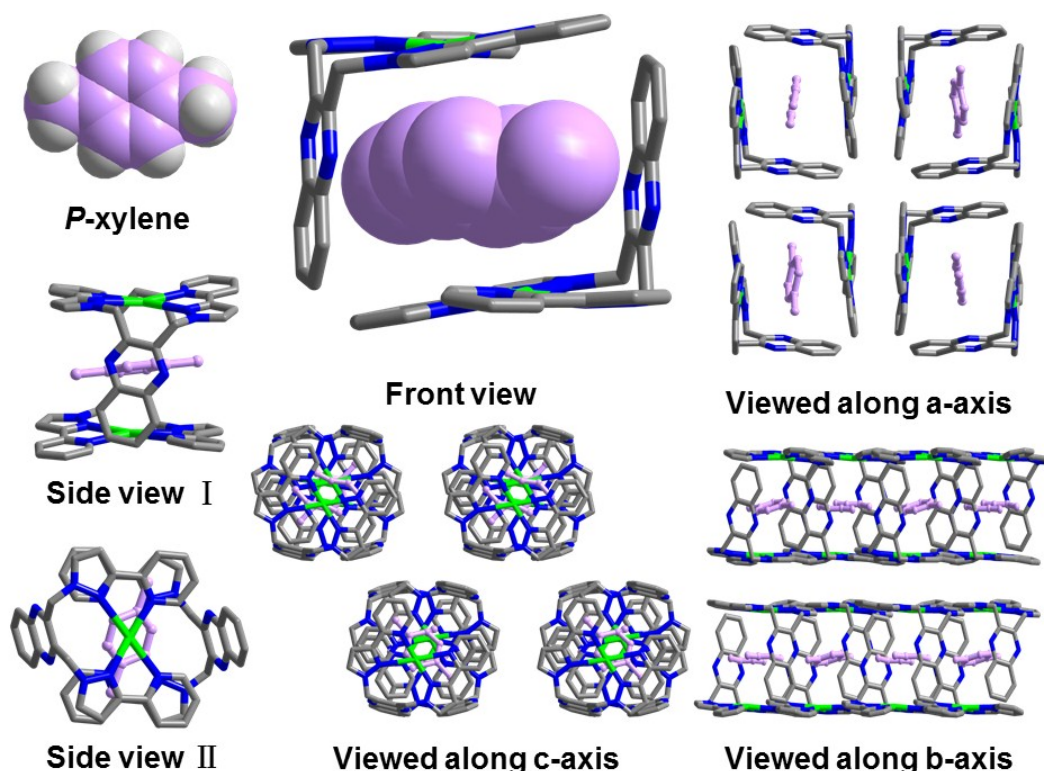


Fig. S3. Different crystallographic views of $pX@M$. Counterions are omitted for clarity.

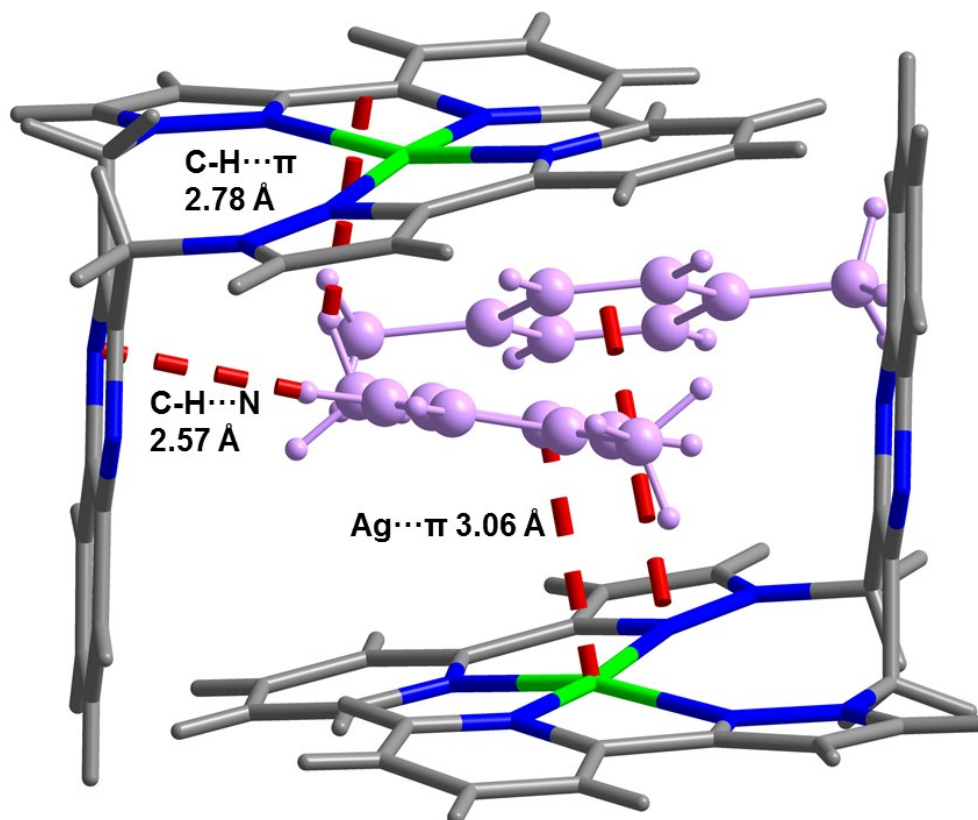


Fig. S4. The guest-loaded phases for pX inside the cage.

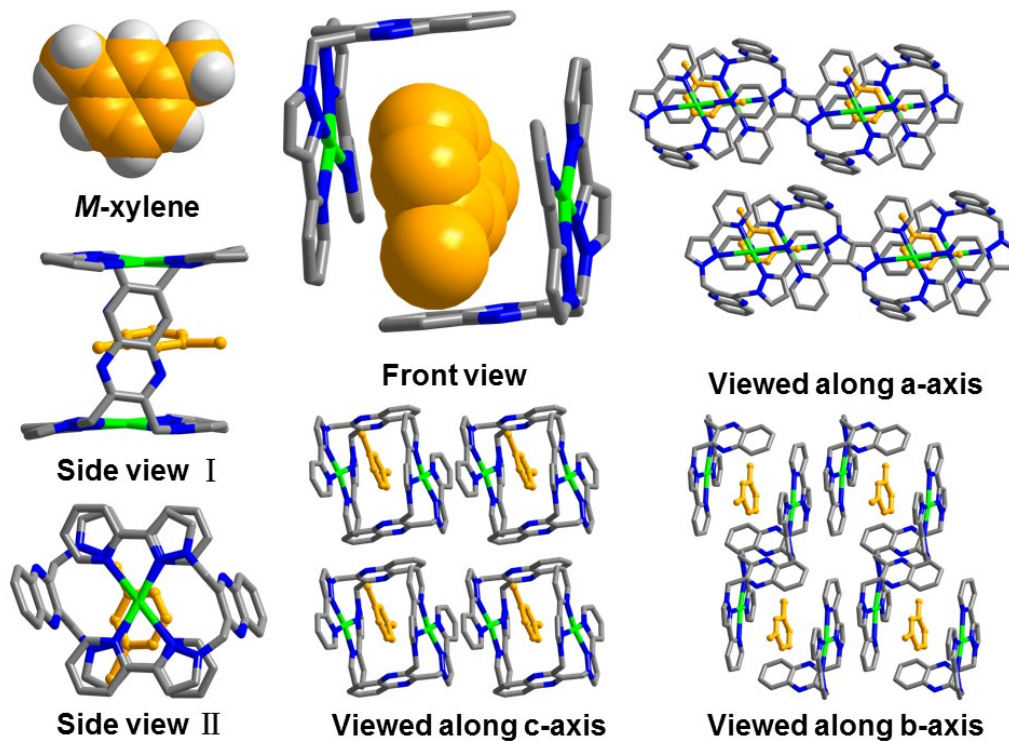


Fig. S5. Different crystallographic views of $mX@M$. Counterions are omitted for the sake of clarity.

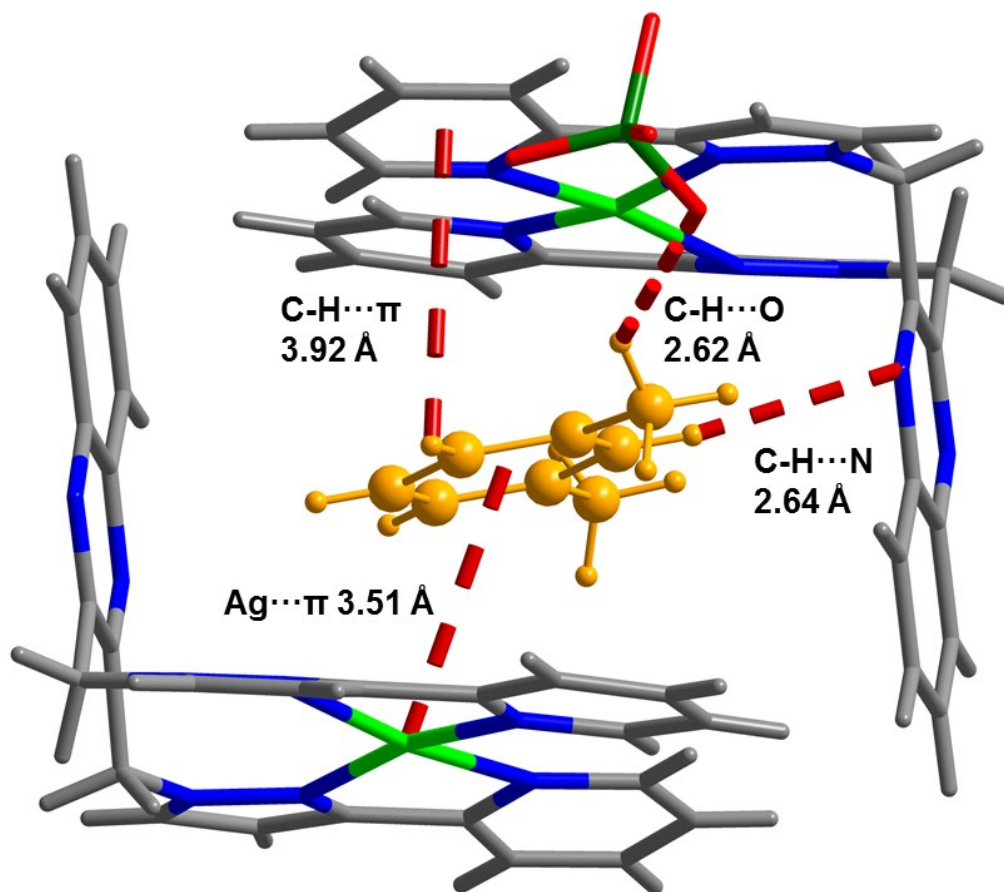


Fig. S6. The guest-loaded phases for *mX* inside the cage.

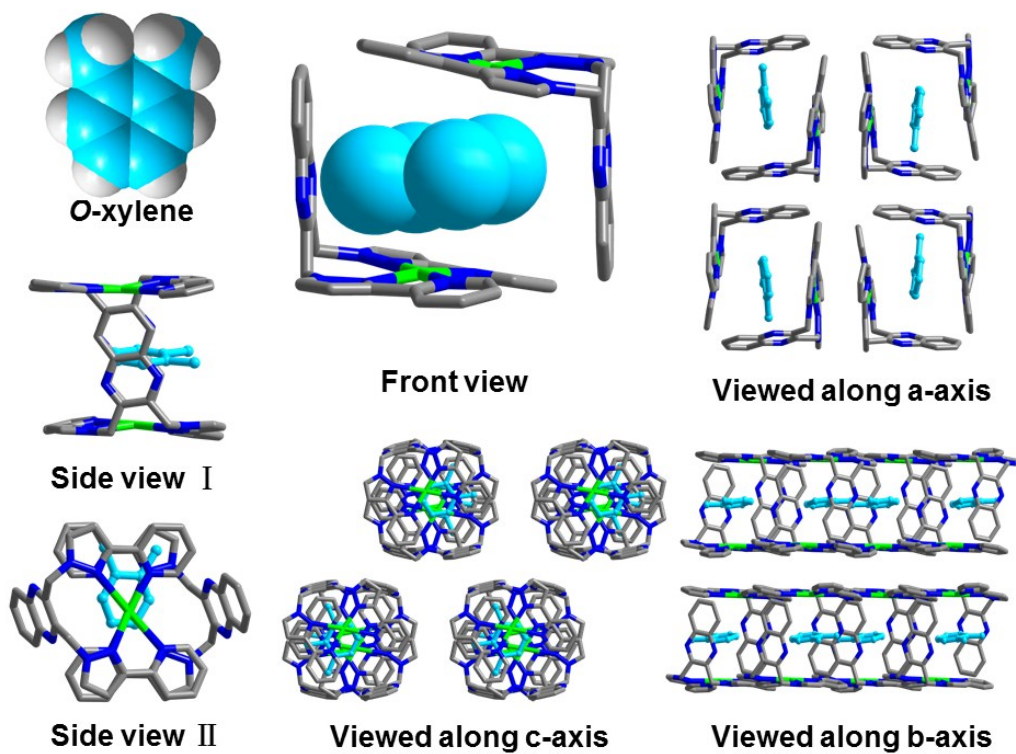


Fig. S7. Different crystallographic views of *oX@M*. Counterions are omitted for the sake of clarity.

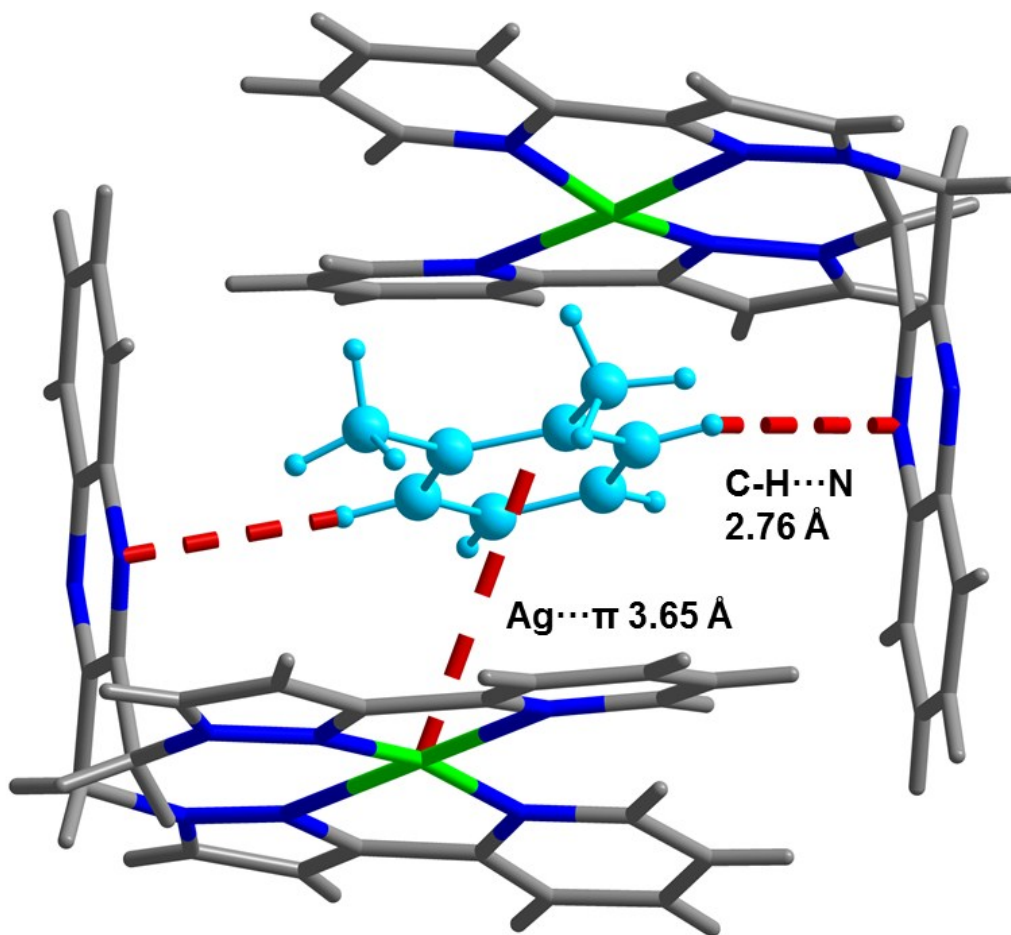


Fig. S8. The guest-loaded phases for *o*X inside the cage.

Section E. Xylene Isomer Selectivity Studies

Solubility of Host in Xylene

The UV absorption spectroscopy (using the corresponding pure xylene as the background) and the ^1H NMR (CDCl_3) experiments of the supernatant after soaking the host **M** in xylenes for 8 hours have been carried out to determine the solubility of the host in xylene, as shown in Fig. S9.

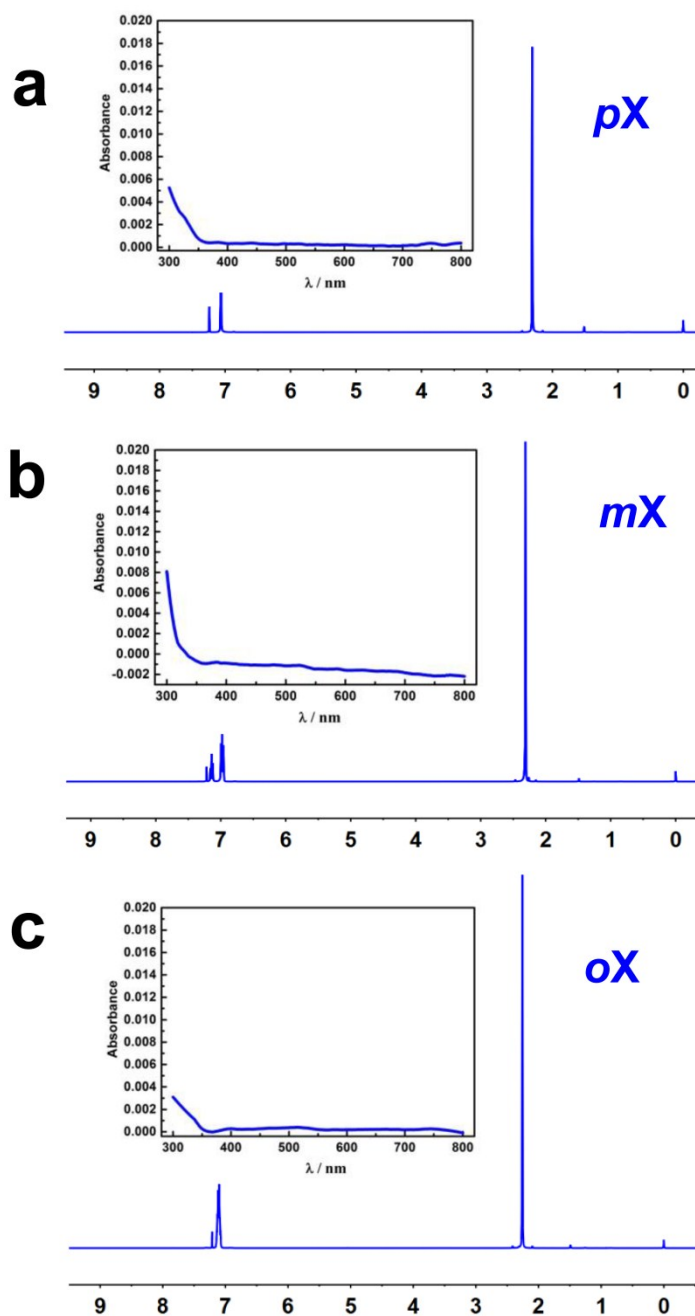


Fig. S9. The UV-vis absorption spectra and the ^1H NMR spectra of the supernatant for *p*X (a), *o*X (b) and *m*X (c) for host **M** soaking in *p*X, *o*X and *m*X, respectively.

Xylene Selectivity Studies in Liquid

About 10 mg of **M** sample was soaked in xylene binary isomer (i.e. *oX/mX*, *oX/pX*, *mX/pX*, 3 mL and commercial grade xylene) separately at the temperature of the liquid was programmed to raise up to 383 K in 6 hours and remained for 2 hours, followed by a cooling program till room temperature in 24 hours, and then powder were collected, air-dried to remove xylenes adhering to the surface of samples. After that, the samples were collected for GC measurements. The GC sample was prepared by 10 mg sample dissolved in 5 mL of DMF. To make it easier to compare, the relevant peaks of xylene isomer are fixed as shown in Table S5.

Table S4. The set values of relevant peaks for the xylene aromatics.

	<i>pX</i>	<i>mX</i>	<i>oX</i>
set value (ppm)	2.26	2.27	2.22
assigned group	2*CH ₃	2*CH ₃	2*CH ₃

a. There are some differences in the experiment because of the different concentrations the interaction.

Table S5. The relevant retention time of the xylene isomers.

	<i>eB</i>	<i>pX</i>	<i>mX</i>	<i>oX</i>
Retention time (min)	7.414	7.776	8.135	10.794

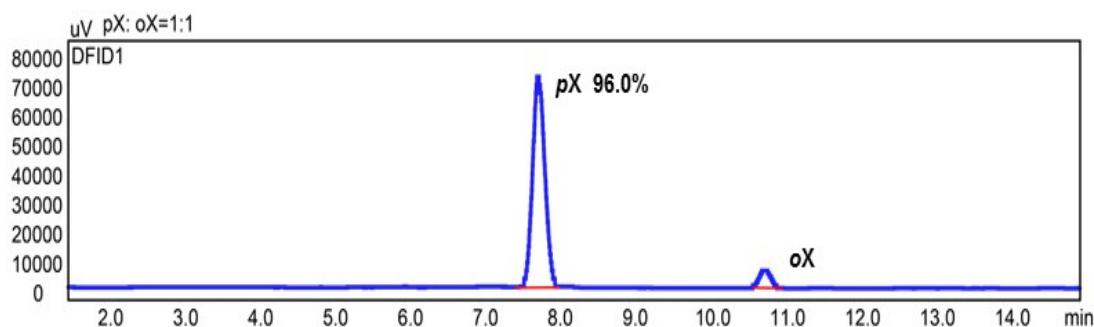


Fig. S10. Relative uptake of xylene isomers (concentration percentage) by **M** after being soaked in a mixture of *pX* and *oX* (1:1, v:v), determined using GC. Any surface adsorbed xylene isomers were removed by air-dried.

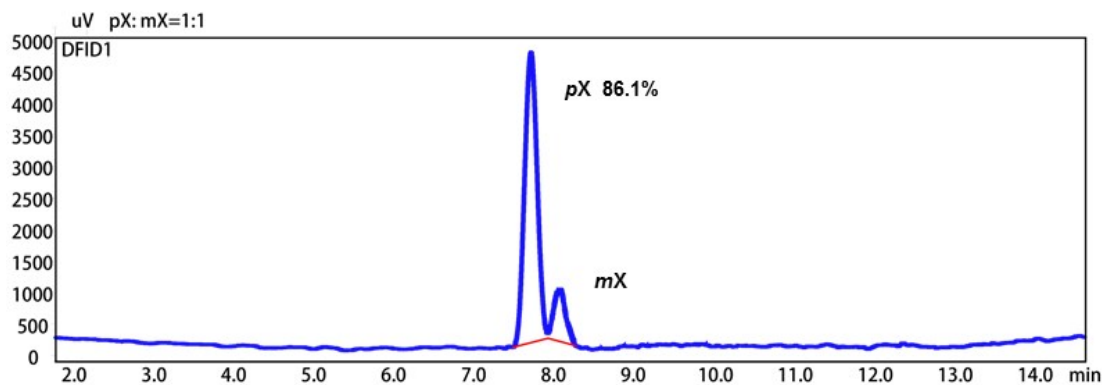


Fig. S11. Relative uptake of xylene isomers (concentration percentage) by **M** after being soak in a mixture of two xylene isomers ($pX:mX=1:1, v:v$), determined using gas chromatography. Any surface adsorbed xylene isomers were removed by air-dried.

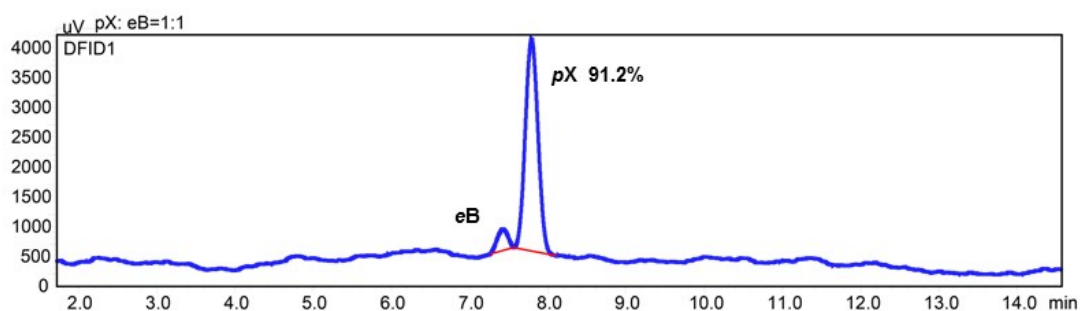


Fig. S12. Relative uptake of xylene isomers (concentration percentage) by **M** after being soak in a mixture of two xylene isomers ($pX:eB=1:1, v:v$), determined using gas chromatography. Any surface adsorbed xylene isomers were removed by air-dried.

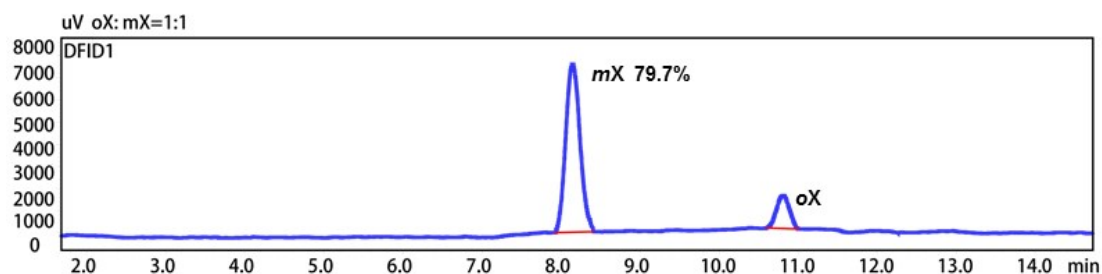


Fig. S13. Relative uptake of xylene isomers (concentration percentage) by **M** after being soak in a mixture of two xylene isomers ($oX:mX=1:1, v:v$), determined using gas chromatography. Any surface adsorbed xylene isomers were removed by air-dried.

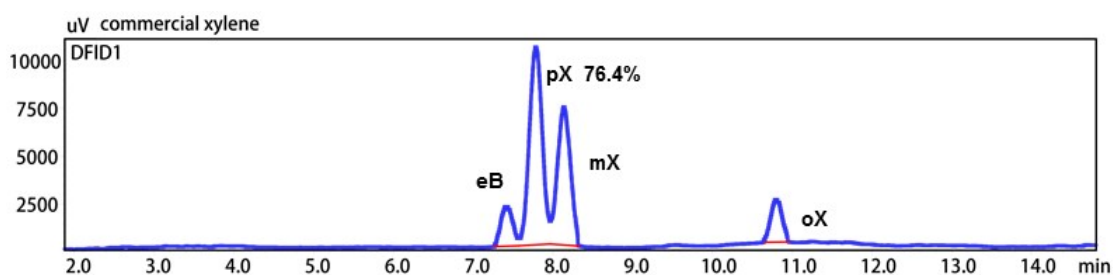


Fig. S14. Relative uptake of xylene isomers (concentration percentage) by **M** after being soak in a Commercial grade xylene, determined using gas chromatography. Any surface adsorbed xylene isomers were removed by air-dried.

Table S6. The concentration percentage of xylene binary isomer in **M** by gas chromatography (liquid, v:v = 1:1)

dimethylbenze	<i>pX</i> (%)	<i>mX</i> (%)	<i>oX</i> (%)	<i>eB</i> (%)
<i>pX</i> : <i>oX</i>	96.0	/	4.0	/
<i>pX</i> : <i>mX</i>	86.1	13.9	/	/
<i>pX</i> : <i>eB</i>	91.2			8.8
<i>oX</i> : <i>mX</i>	/	79.7	20.3	/
Commercial xylene	76.4	13.2	2.8	7.63

Table S7. Selectivity calculated for **M** uptaking mixtures (v:v = 1:1) of xylene isomer. Seletivities (α_{ij}) are calculated using the uptake of the compound *i* in the top row over the uptake of compound *j* in the second column (in liquid, the average at least 5 times).

Adsorbent	<i>Isomer j</i>	<i>Isomer i</i>			
		<i>pX</i>	<i>mX</i>	<i>oX</i>	<i>eB</i>
M(current work)	<i>pX</i>	/	0.16	0.03	0.09
	<i>mX</i>	6.19	/	0.25	/
	<i>oX</i>	24.0	3.93	/	/
	<i>eB</i>	10.36	/	/	/

Recycled of **M**

After the **M** soaking or exposing in xylene isomers later, it was collected, laid on a weighing paper, placed in a vacuum oven at a temperature of 60 degrees, and 12 hours later, the sample was taken out and carried out ¹H NMR and PXRD. The results are shown in the Fig. S19.

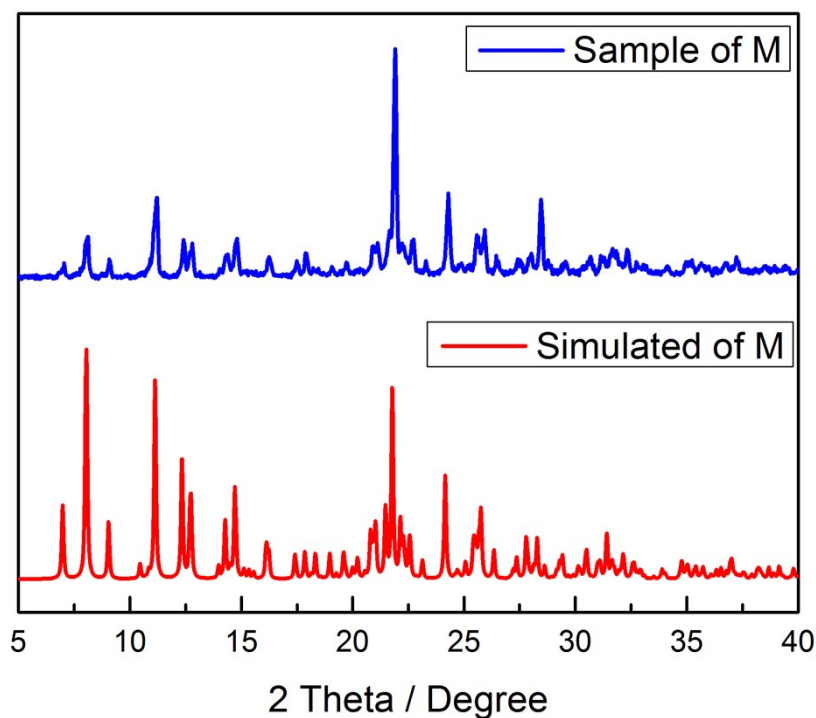


Fig. S15. The sample of $pX@M$ after vacuum drying and the simulated of **M**.

Xylene Selectivity Studies in Vapor

About 100 mg of **M** sample was put in xylene binary isomer vapor (i.e. oX/mX , oX/pX , mX/pX , 2 mL) separately at room temperature in vacuum for 24 hours. When each sample exposed 24 hours later, they were taken out, air-dried to remove xylenes adhering to the surface of samples. After that, the samples were collected for GC measurements. The GC sample was prepared by 10 mg sample dissolved in 5 mL of DMF. To make it easier to compare, the relevant peaks of xylene isomer are fixed as shown in Table S5.

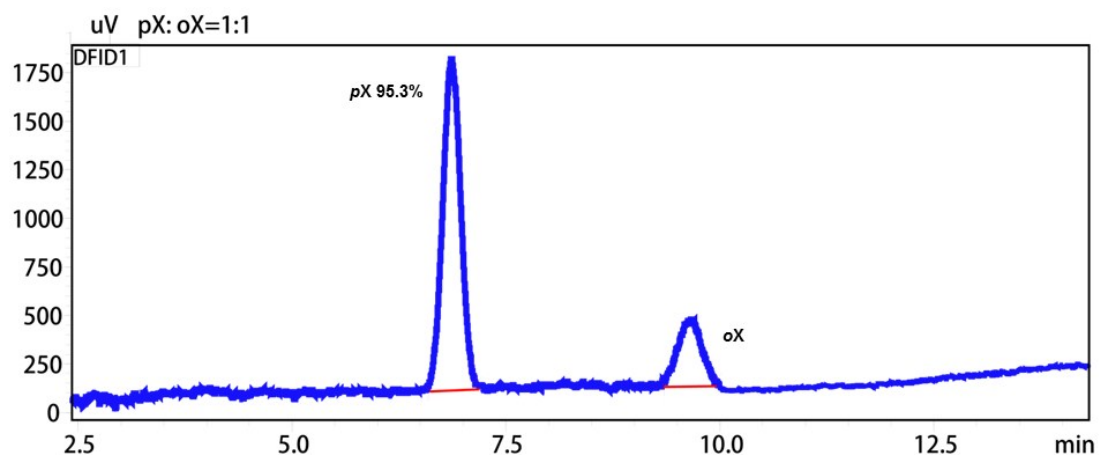


Fig. S16. Relative uptake of xylene isomers (concentration percentage) by **M** after being vaporized in a mixture of *pX* and *oX* (1:1, v:v) for 24 hours at 298 K, determined using GC. Any surface adsorbed xylene isomers were removed by air-dried.

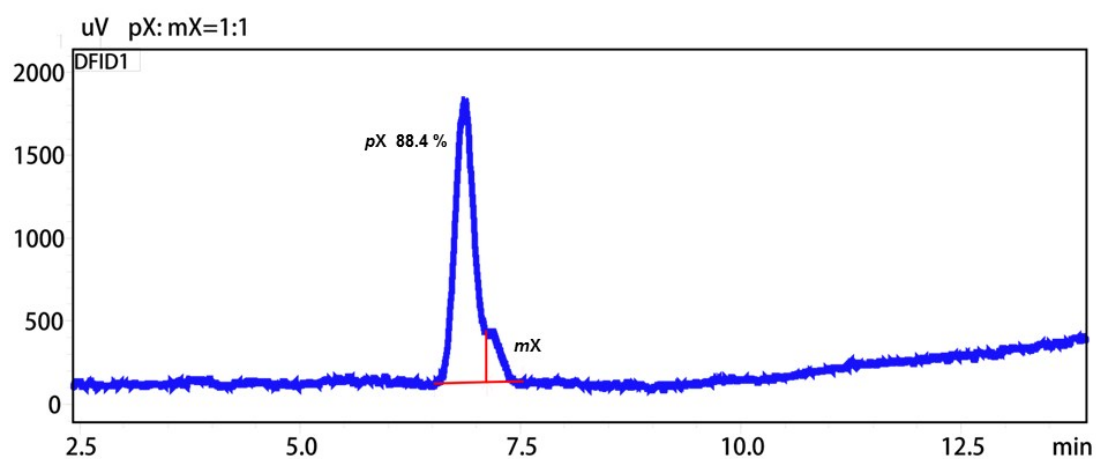


Fig. S17. Relative uptake of xylene isomers (concentration percentage) by **M** after being vaporized in a mixture of *pX* and *mX* (1:1, v:v) for 24 hours at 298 K, determined using GC. Any surface adsorbed xylene isomers were removed by air-dried.

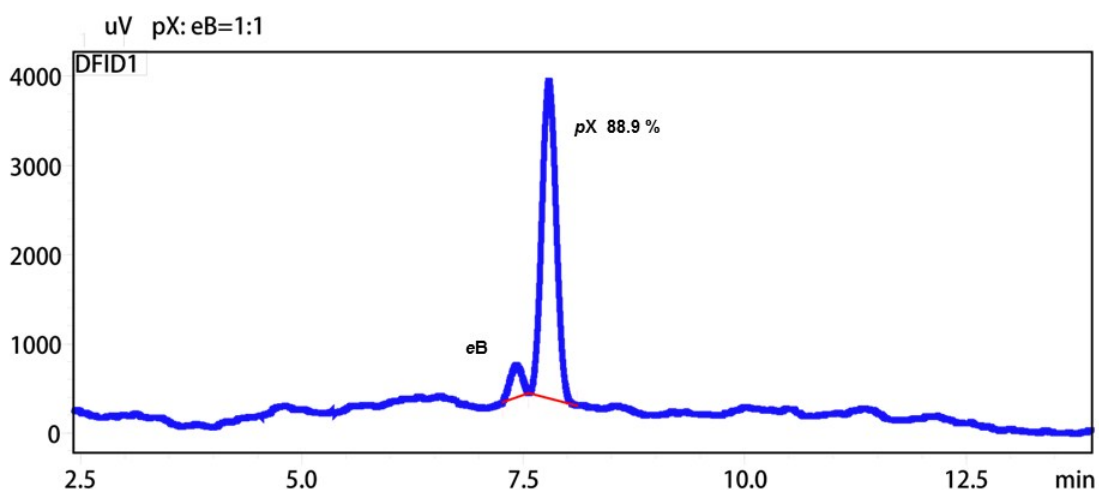


Fig. S18. Relative uptake of xylene isomers (concentration percentage) by **M** after being vaporized in a mixture of *p*X and *e*B (1:1, v:v) for 24 hours at 298 K, determined using GC. Any surface adsorbed xylene isomers were removed by air-dried.

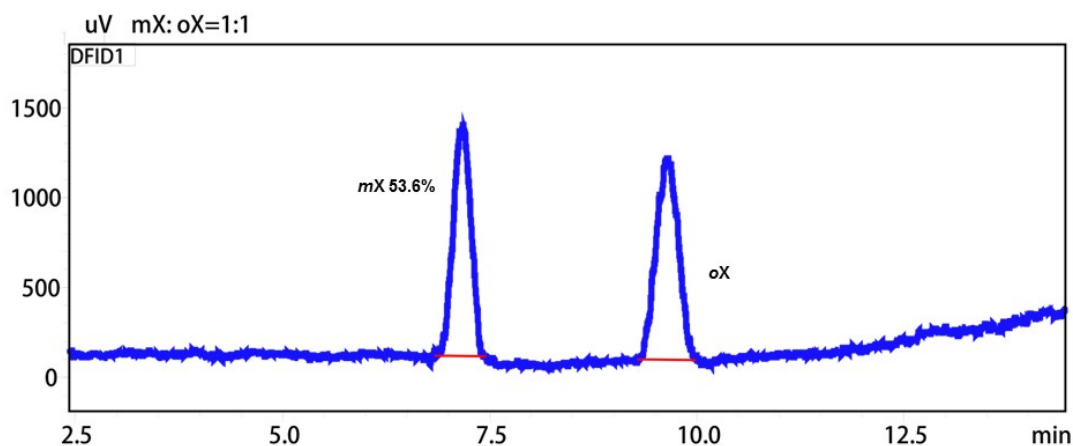


Fig. S19. Relative uptake of xylene isomers (concentration percentage) by **M** after being vaporized in a mixture of *m*X and *o*X (1:1, v:v) for 24 hours at 298 K, determined using GC. Any surface adsorbed xylene isomers were removed by air-dried.

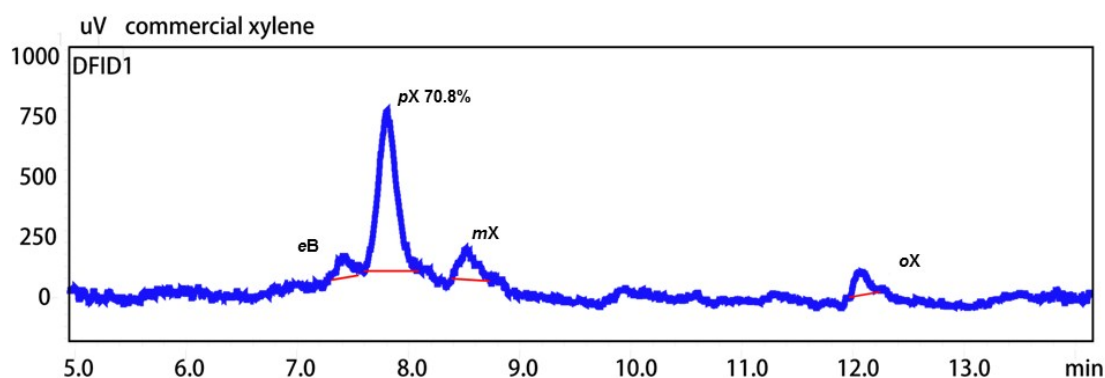


Fig. S20. Relative uptake of xylene isomers (concentration percentage) by **M** after being vaporized in a Commercial grade xylene for 24 hours at 298K, determined using gas chromatography. Any surface adsorbed xylene isomers were removed by air-dried.

Table S8. The concentration percentage of xylene binary isomer in **M** by gas chromatography (**vapor**, v:v = 1:1)

dimethylbenzene	<i>p</i> X(%)	<i>m</i> X(%)	<i>o</i> X(%)	<i>e</i> B(%)
<i>p</i> X: <i>o</i> X	95.3	/	4.7	/
<i>p</i> X: <i>m</i> X	84.4	15.6	/	/
<i>p</i> X: <i>e</i> B	88.9			11.1
<i>o</i> X: <i>m</i> X	/	53.6	46.4	/

Commercial xylene	70.8	10.6	13	5.5
-------------------	-------------	------	----	-----

Table S9. Selectivity calculated for **M** uptaking mixtures (v:v = 1:1) of xylene isomer. Selectivities (α_{ij}) are calculated using the uptake of the compound *i* in the top row over the uptake of compound *j* in the second column (in vapor, the average at least 5 times).

Adsorbent	Isomer <i>j</i>	Isomer <i>i</i>			
		<i>pX</i>	<i>mX</i>	<i>oX</i>	<i>eB</i>
M(current work)	<i>pX</i>	/	0.18	0.05	0.12
	<i>mX</i>	5.41	/	0.87	/
	<i>oX</i>	20.28	1.16	/	/
	<i>eB</i>	8.00	/	/	/

DFT Calculations

The complexation energy E_{ce} was defined as:

$$E_{ce} = E(\text{complex}) - E(\text{host}) - E(\text{inserted xylene}) - E(\text{BSSE})$$

Where, $E(\text{complex})$, $E(\text{host})$, $E(\text{inserted xylene})$ denotes the energy of host- inserted xylene complex, host, and xylene, respectively, while $E(\text{BSSE})$ denotes the basis set superposition errors. Based on the DFT calculations, the complexation energy was predicted for the supramolecular systems (in WB97XD functional,³³ using Gaussian 09 program package³⁴), and the start geometries of host-guest supramolecular system were deduced from the single crystal structure data. Further optimization was carried out only for the inserted xylene isomer with the host structure frozen. The obtained optimized structure was used for complexation energy (E_{ce}) calculations with the consideration of BSSE correction³⁵, where aug-cc-pvdz-pp^{36,37} pseudo potential basis sets was used for Ag and 6-31+g(d,p) basis sets for C, H and N atoms. As shown in Table S10, the complexation energy for *pX@M* is larger than those of *oX@M* and *mX@M*.

Table S10. The different binding energy of *pX@M*, *mX@M*, *oX@M*.

Binding energy	<i>pX@M</i>	<i>mX@M</i>	<i>oX@M</i>
E_{CE} (kCal/mol)	34.61	31.05	32.99

Section F. Main Bond Length and Bond Angle

Main hydrogen bond of $oX@M$ and $mX@M$ and $pX@M$ length (Å) and bond angle (°) tables

Table S11. Clathrate $pX@M$ main hydrogen bond length (Å) and bond angle (°) tables

D-H	d(D-H)	d(H..A)	<DHA	d(D..A)	A
C27-H27	0.930	2.637	130.74	3.320	O7 [x-1, y, z]
C32-H32B	0.970	2.646	173.86	3.612	O1 [x-1/2, -y+3/2, z-1/2]
C42-H42	0.930	2.657	116.14	3.179	O7
C43-H43	0.930	2.648	145.82	3.457	O3 [-x+2, -y+2, -z+1]
C51-H51	0.930	2.545	136.36	3.281	O6 [-x+2, -y+1, -z+1]
C53-H53	0.930	2.626	167.13	3.539	O2 [-x+3/2, y-1/2, -z+3/2]
C58-H58B	0.970	2.577	149.80	3.450	O5 [x-1/2, -y+3/2, z+1/2]
C67-H67A	0.970	2.489	163.22	3.429	O4
C68-H68	0.930	2.480	136.54	3.219	O1
C72-H72	0.930	2.657	133.94	3.369	O7 [x+1/2, -y+3/2, z+1/2]

Table S12. Clathrate $mX@M$ main hydrogen bond length (Å) and bond angle (°) tables

D-H	d(D-H)	d(H..A)	<DHA	d(D..A)	A
C6-H6	0.930	2.654	166.58	3.565	O3 [-x, -y+1, -z+2]
C9-H9	0.930	2.531	167.04	3.444	O3 [x+1, y-1, z]
C13-H13	0.930	2.989	137.77	3.730	Cl1 [-x+1, -y+1, -z+1]
C13-H13	0.930	2.578	163.52	3.479	O3 [-x+1, -y+1, -z+1]
C18-H18B	0.970	2.628	117.05	3.189	O4 [-x+1, -y+1, -z+2]
C25-H25	0.930	2.608	156.15	3.479	O2 [-x+1, -y+2, -z+1]

Table S13. Clathrate $oX@M$ main hydrogen bond length (Å) and bond angle (°) tables

D-H	d(D-H)	d(H..A)	<DHA	d(D..A)	A
C30-H30	0.930	2.602	163.90	3.505	O5 [x, -y+3/2, z+1/2]
C44-H44B	0.970	2.533	162.68	3.471	O7 [-x+1, -y+1, -z+1]
C45-H45	0.930	2.424	138.62	3.181	O6 [-x+1, -y+1, -z+1]
C49-H49	0.930	2.598	137.42	3.342	O3 [-x+2, -y+1, -z+1]
C4-H4	0.930	2.657	127.30	3.305	O6 [x+1, y, z]
C9-H9B	0.970	2.553	148.13	3.416	O4 [-x+2, y+1/2, -z+1/2]
C18-H18A	0.970	2.628	170.26	3.587	O6 [-x+1, y+1/2, -z+1/2]
C23-H23	0.930	2.606	135.45	3.334	O3 [-x+1, y+1/2, -z+1/2]

Table S14. M main bond length (Å) and bond angle (°) tables

Ag(1)-N(7)	2.700(5)	Ag(1)-N(5)	2.667(6)
Ag(1)-N(4)	2.152(6)	Ag(1)-N(8)	2.206(6)
N(7)-Ag(1)-N(5)	170.8(2)	N(7)-Ag(1)-N(4)	118.7(2)
N(5)-Ag(1)-N(4)	70.4(2)	N(4)- Ag(1)-N(8)	162.8(2)
N(5)-Ag(1)-N(8)	102.8(2)	N(7)- Ag(1)-N(8)	68.0(2)

Table S15. Clathrate *pX*@M main bond length (Å) and bond angle (°) tables

Ag(1)-N(4)	2.723(3)	Ag(1)-N(5)	2.179(3)
Ag(1)-N(7)	2.162(3)	Ag(1)-N(8)	2.688(3)
N(5)-Ag(1)-N(4)	69.01(10)	N(5)-Ag(1)-N(8)	108.06(11)
N(7)-Ag(1)-N(4)	113.84(10)	N(7)- Ag(1)-N(5)	176.57(12)
N(7)-Ag(1)-N(8)	68.91(11)	N(8)- Ag(1)-N(4)	173.74(10)

Table S16. Clathrate *mX*@M main bond length (Å) and bond angle (°) tables

Ag(1)-N(4)	2.723(3)	Ag(1)-N(5)	2.179(3)
Ag(1)-N(7)	2.162(3)	Ag(1)-N(8)	2.688(3)
N(5)-Ag(1)-N(4)	69.01(10)	N(5)-Ag(1)-N(8)	108.06(11)
N(7)-Ag(1)-N(4)	113.84(10)	N(7)- Ag(1)-N(5)	176.57(12)
N(7)-Ag(1)-N(8)	68.91(11)	N(8)- Ag(1)-N(4)	173.74(10)

Table S17. Clathrate *oX*@M main bond length (Å) and bond angle (°) tables

Ag(1)-N(4)	2.723(3)	Ag(1)-N(5)	2.179(3)
Ag(1)-N(7)	2.162(3)	Ag(1)-N(8)	2.688(3)
N(5)-Ag(1)-N(4)	69.01(10)	N(5)-Ag(1)-N(8)	108.06(11)
N(7)-Ag(1)-N(4)	113.84(10)	N(7)- Ag(1)-N(5)	176.57(12)
N(7)-Ag(1)-N(8)	68.91(11)	N(8)- Ag(1)-N(4)	173.74(10)

Section G. References

- (1) Sheldrick, G. M. *Acta Crystallogr. Sect. A*, 2008, **64**, 112.
- (2) Zou, R. Q.; Liu, C. S.; Huang, Z.; Hu, T. L.; Bu, X. H. *Crystal Growth & Design*, 2006, **6**, 99.
- (3) Rasouli, M.; Yaghobi, N.; Chitsazan, S.; Sayyar, M. H. *Microporous Mesoporous Mater.*, 2012, **150**, 47.
- (4) Jie, K.; Liu, M.; Zhou, Y.; Little, M. A.; Pulido, A.; Chong, S. Y.; Stephenson, A.; Hughes, A. R.; Sakakibara, F.; Ogoshi, T.; Blanc, F.; Day, G. M.; Huang, F.; Cooper, A. I. *J. Am. Chem. Soc.*, 2018, **140**, 6921.
- (5) Warren, J. E.; Perkins, C. G.; Jelfs, K. E.; Boldrin, P.; Chater, P. A.; Miller, G. J.; Manning, T. D.; Briggs, M. E.; Stylianou, K. C.; Claridge, J. B.; Rosseinsky, M. J. *Angew. Chem. Int. Ed.*, 2014, **53**, 4592.
- (6) Gu, Z.-Y.; Jiang, D.-Q.; Wang, H.-F.; Cui, X.-Y.; Yan, X.-P. *J. Phys. Chem. C*, 2010, **114**, 311.
- (7) Peralta, D.; Chaplais, G.; Paillaud, J.-L.; Simon-Masseron, A.; Barthelet, K.; Pirngruber, G. D. *Microporous Mesoporous Mater.*, 2013, **173**, 1.
- (8) Rasouli, M.; Yaghobi, N.; Allahgholipour, F.; Atashi, H. *Chem. Een. Res. Ded.*, 2014, **92**, 1192.
- (9) Rasouli, M.; Yaghobi, N.; Gilani, S. Z. M.; Atashi, H.; Rasouli, M. *Chinese. J. Chem. Eng.*, 2015, **23**, 64.
- (10) Vermoortele, F.; Maes, M.; Moghadam, P. Z.; Lennox, M. J.; Ragon, F.; Boulhout, M.; Biswas, S.; Laurier, K. G. M.; Beurroies, I.; Denoyel, R.; Roeffaers, M.; Stock, N.; Düren, T.; Serre, C.; De Vos, D. E. *J. Am. Chem. Soc.*, 2011, **133**, 18526.
- (11) Gee, J. A.; Zhang, K.; Bhattacharyya, S.; Bentley, J.; Rungta, M.; Abichandani, J. S.; Sholl, D. S.; Nair, S. *J. Phys. Chem. C*, 2016, **120**, 12075.
- (12) Lin, J.-M.; He, C.-T.; Liao, P.-Q.; Lin, R.-B.; Zhang, J.-P. *Sci. Rep.*, 2015, **5**, 11537.
- (13) Finsy, V.; Verelst, H.; Alaerts, L.; De Vos, D.; Jacobs, P. A.; Baron, G. V.; Denayer, J. F. M. *J. Am. Chem. Soc.*, 2008, **130**, 7110.
- (14) Peralta, D.; Barthelet, K.; Pérez-Pellitero, J.; Chizallet, C.; Chaplais, G.; Simon-Masseron, A.; Pirngruber, G. D. *J. Phys. Chem. C*, 2012, **116**, 21844.
- (15) Alaerts, L.; Kirschhock, C. E. A.; Maes, M.; van der Veen, M. A.; Finsy, V.; Depla, A.; Martens, J. A.; Baron, G. V.; Jacobs, P. A.; Denayer, J. E. M.; De Vos, D. E. *Angew. Chem. Int. Ed.*, 2007, **46**, 4293.
- (16) Niekiet, F.; Lannoeye, J.; Reinsch, H.; Munn, A. S.; Heerwig, A.; Zizak, I.; Kaskel, S.; Walton, R. I.; de Vos, D.; Llewellyn, P.; Lieb, A.; Maurin, G.; Stock, N. *Inorg. Chem.*, 2014, **53**, 4610.
- (17) Trens, P.; Belarbi, H.; Shepherd, C.; Gonzalez, P.; Ramsahye, N. A.; Lee, U. H.; Seo, Y.-K.; Chang, J.-S. *Microporous Mesoporous Mater.*, 2014, **183**, 17.
- (18) Gu, Z.-Y.; Yan, X.-P. *Angew. Chem. Int. Ed.*, 2010, **49**, 1477.
- (19) Nicolau, M. P. M.; B arcia, P. S.; Gallegos, J. M.; Silva, J. A. C.; Rodrigues, A. E.; Chen, B. *J. Phys. Chem. C*, 2009, **113**, 13173.
- (20) El Osta, R.; Carlin-Sinclair, A.; Guillou, N.; Walton, R. I.; Vermoortele, F.; Maes, M.; de Vos, D.; Millange, F. *Chem. Mater.*, 2012, **24**, 2781.
- (21) Agrawal, M.; Bhattacharyya, S.; Huang, Y.; Jayachandrababu, K. C.; Murdock, C. R.; Bentley, J. A.; Rivas-Cardona, A.; Mertens, M. M.; Walton, K. S.; Sholl, D. S.; Nair, S. *J. Phys. Chem. C*, 2018, **122**, 386.

- (22) Alaerts, L.; Maes, M.; Giebel, L.; Jacobs, P. A.; Martens, J. A.; Denayer, J. F. M.; Kirschhock, C. E. A.; De Vos, D. E. *J. Am. Chem. Soc.*, 2008, **130**, 14170.
- (23) Gonzalez, M. I.; Kapelewski, M. T.; Bloch, E. D.; Milner, P. J.; Reed, D. A.; Hudson, M. R.; Mason, J. A.; Barin, G.; Brown, C. M.; Long, J. R. *J. Am. Chem. Soc.*, 2018, **140**, 3412.
- (24) Wang, S.-Q.; Mukherjee, S.; Patyk-Kazmierczak, E.; Darwish, S.; Bajpai, A.; Yang, Q.-Y.; Zaworotko, M. J. *Angew. Chem. Int. Ed.*, 2019, **58**, 6630.
- (25) Lusi, M.; Barbour, L. J. *Angew. Chem. Int. Ed.*, 2012, **51**, 3928.
- (26) Finsy, V.; Kirschhock, C. E. A.; Vedts, G.; Maes, M.; Alaerts, L.; De Vos, D. E.; Baron, G. V.; Denayer, J. F. M. *Chem.-Eur. J.*, 2009, **15**, 7724.
- (27) Moreira, M. A.; Santos, J. C.; Ferreira, A. F. P.; Loureiro, J. M.; Ragon, F.; Horcajada, P.; Shim, K.-E.; Hwang, Y.-K.; Lee, U. H.; Chang, J.-S.; Serre, C.; Rodrigues, A. E. *Langmuir*, 2012, **28**, 5715.
- (28) Rasouli, M.; Yaghobi, N.; Chitsazan, S.; Sayyar, M. H. *Microporous Mesoporous Mater.*, 2012, **152**, 141.
- (29) Daver, H.; Algarra, A. G.; Rebek, J., Jr.; Harvey, J. N.; Himo, F. *J. Am. Chem. Soc.*, 2018, **140**, 12527.
- (30) Mantooth, S. M.; Munoz-Robles, B. G.; Webber, M. J. *Macromol. Biosci.*, 2019, **19**.
- (31) Hong, C. M.; Bergman, R. G.; Raymond, K. N.; Toste, F. D. *Acc. Chem. Res.*, 2018, **51**, 2447.
- (32) Wang, F.; Han, Y.; Lim, C. S.; Lu, Y.; Wang, J.; Xu, J.; Chen, H.; Zhang, C.; Hong, M.; Liu, X. *Nature*, 2010, **463**, 1061.
- (33) Chai, J.-D.; Head-Gordon, M. *Phys. Chem. Chem. Phys.*, 2008, **10**, 6615.
- (34) Curtiss, L. A.; Redfern, P. C.; Raghavachari, K.; Pople, J. A. *J. Chem. Phys.*, 1998, **109**, 42.
- (35) Salvador, P.; Paizs, B.; Duran, M.; Suhai, S. *J. Comput. Chem.*, 2001, **22**, 765.
- (36) Peterson, K. A.; Puzzarini, C. *Theor. Chem. Acc.*, 2005, **114**, 283.
- (37) Figgen, D.; Rauhut, G.; Dolg, M.; Stoll, H. *Chem. Phys.*, 2005, **311**, 227.